Polymer 50 (2009) 4056–4065

Contents lists available at ScienceDirect

Polymer

journal homepage: www.elsevier.com/locate/polymer

Understanding of scratch-induced damage mechanisms in polymers

Han Jiang, Robert Browning, Hung-Jue Sue*

Polymer Technology Center, Department of Mechanical Engineering, Texas A&M University, College Station, TX 77843-3123, USA

ARTICLE INFO

Article history:
Received 28 March 2009
Received in revised form
9 June 2009
Accepted 11 June 2009
Available online 30 June 2009

Keywords:
Scratch map
Polymer
Damage mode

ABSTRACT

Following the ASTM and ISO test standards, a series of scratch tests were carried out on four categories of polymers: I) ductile and strong, II) ductile and weak, III) brittle and weak, and IV) brittle and strong. The scratch damage features were characterized by using a desktop scanner for scratch visibility assessment, and optical and electron microscopes for detailed damage mechanisms investigation. Various scratch damage mechanisms were identified for the different categories of polymers. The effect of testing rate on possible alteration of scratch damage mechanisms was also studied. The stress fields experienced by the polymer during scratch were determined using three-dimensional finite element methods modeling. It is found that both the material characteristics and the complex stress state exerted on the scratched surface are responsible for the various scratch damage mechanisms observed. A generalized scratch damage mechanism map for polymers is presented. The usefulness of the above understanding for designing scratch-resistant polymers is also discussed.

Published by Elsevier Ltd.

1. Introduction

The scratch performance of polymers has caught significant attention in the past few years because of their greatly expanded usage in the electronic, optical, household, and automotive applications where long-term aesthetics is important. Unlike ceramics and metals, polymers are particularly susceptible to surface deformation and damage, even under low contact loads. The scratch process herein is defined as a mechanical deformation process where a controlled force or displacement is exerted on a hard spherical tip to indent onto a polymer substrate and move across its surface at a prescribed speed.

It should be noted that the scratch tip geometry, tip material, substrate thickness and surface characteristics, and rate of testing can all significantly affect the scratch performance of polymers. Extensive research efforts have been dedicated to the development of an objective test methodology for polymer scratch [1–9]. This has led to the establishment of an ASTM and ISO standard [1,2] for scratch testing of polymers, from which more in-depth description of the standardized polymer scratch testing can be found. The recommended progressive scratch load test appears to be a promising method for systematic fundamental study and evaluation of the polymer scratch behaviors.

Scratch-induced deformation of polymers is a complex mechanical process. The nonlinear material characteristics and complex scratch-induced stress fields have made it extremely difficult to gain fundamental knowledge of polymer scratch behavior. Generally speaking, there are two main types of damage found in polymers: ductile damage (e.g., shear yielding and ironing) and brittle damage (e.g., crazing and cracking); their occurrence depends on the material characteristics and applied stress state and magnitude [10,11]. In addition, debonding and voiding can take place if the polymer contains inclusion phases, such as talc and rubber. Various scratch-induced damage features, such as mar, fish-scale, parabolic crack, and material removal, have been observed from a wide variety of polymeric materials [12–18]. The effect of surface friction on polymer scratch behavior has been investigated [18–20]. The role of additives in polymer scratch resistance has been probed [6,7,20–22]. Attempts have been made to create a deformation and damage map for polymer scratch [23–25]. Research efforts have also been focused on testing rate and temperature effect on scratch behaviors [26,27]. While the above research efforts have provided valuable knowledge within their own merits, they lack a comprehensive understanding of how the material parameters influence the scratch behavior, especially the formation of scratch-induced damage features. Consequently, correlation between the material properties and the scratch mechanics has to be established to allow for better description and prediction of scratch-induced damage mechanisms and their evolution processes based on the ASTM/ISO standard.

Numerical analysis has been utilized to investigate the mechanics associated with the damage features incurred during polymer scratch. While molecular dynamics (MD) simulations are chosen for understanding of nano-scale scratch phenomena [28,29], numerical simulation approaches, such as finite element

* Corresponding author.
E-mail address: hjsue@tamu.edu (H.-J. Sue).

0032-3861/$ – see front matter Published by Elsevier Ltd.
doi:10.1016/j.polymer.2009.06.061

method (FEM), are utilized for modeling scratch behavior on the micro- or macro- level. Previous FEM simulation efforts on this topic remain scant and are restricted to linear elastic – perfect plastic materials or to two-dimensional (2-D) plane-strain problems. Recently, with greatly improved computational capabilities, three-dimensional (3D) FEM analyses become viable for polymer scratch research [30–33]. Nevertheless, in addition to the classical mechanics complexities, there are still other challenges, such as utilization of a realistic polymers material constitutive model and choice of appropriate criteria for various scratch-induced damage mechanisms. Although FEM simulations still face significant challenges for successful modeling of realistic polymer scratch behavior and provide accurate predictions, it has been shown to be effective for phenomenological description of polymer scratch process and for establishment of qualitative correlation between material properties and the observed damage features.

To aid the design of scratch-resistant polymers, knowledge on the evolution of the damage process and its corresponding mechanics and material properties are essential. In this paper, scratch tests were performed on four general types of polymers which are classified as: (I) ductile and strong, (II) ductile and weak, (III) brittle and weak, and (IV) brittle and strong. The scratch tests were also conducted at different rates on ethylene–propylene rubber (EPR) rich soft thermoplastic olefins (TPO) to investigate how the damage process is affected by rate of testing. The observed damage features were identified and classified according to its material type. 3D FEM numerical modeling was performed to explore the mechanistic reasons responsible for the observed damage mechanisms. With the help of material science and mechanics tools, a better understanding of the relationship between the scratch damage process and material properties is obtained and summarized as a scratch damage evolution map. Approach to design scratch-resistant polymers is discussed.

2. Experiment details

2.1. Model materials

To study the scratch behavior of polymers, four typical commercially available polymers were chosen for the present study and are categorized as: (I) ductile and strong (polycarbonate (PC); Lexan 9034, GE Plastics); (II) ductile and weak (TPO with 70% polypropylene and 30% ethylene–propylene rubber (EPR), Advanced Composites); (III) brittle and weak (polystyrene (PS), Styron 685D, Dow Chemical); (IV) brittle and strong (Epoxy, DER 332, Dow Chemical). Here, the strong polymers typify those polymers that exhibit high modulus and high ultimate tensile strength. On the contrary, the weak polymers possess low modulus and low tensile strength. The ductile polymers can experience much larger tensile elongation before failure than the brittle ones. Schematic of the typical stress–strain curves of the four categories of polymers are shown in Fig. 1.

To study the rate effect on polymer scratch behavior, a soft TPO with a high concentration of EPR (30% PP + 70% EPR, Sumitomo Chemical, Ltd.) was also investigated.

All samples possess smooth surface characteristics with 50 mm in length, 10 mm in width, and 3 mm in thickness. The sample surfaces were cleaned by an air duster prior to the scratch tests.

2.2. Scratching machine and test conditions

Following the ASTM and ISO testing standard for polymer scratch [1,2,9], a custom-built scratch machine (Surface Machine Systems, LLC) is utilized to perform the scratch tests at ambient condition (Fig. 2). The machine is capable of recording tangential and normal forces as well as scratch distance and instantaneous depth experienced by the stylus.

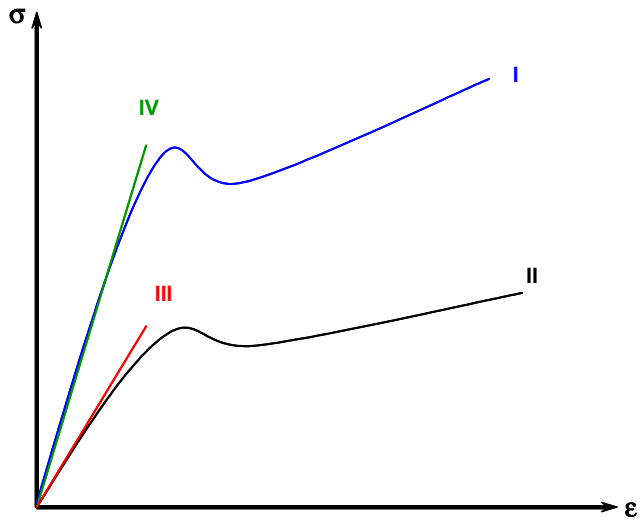

Fig. 1. Schematic stress–strain curves of four categories of polymers: (I) ductile & strong; (II) ductile & weak; (III) brittle & weak; and (IV) brittle & strong.

A stainless steel spherical tip with 1 mm in diameter was used for the weak polymers and soft TPO; a tungsten carbide spherical tip with 1 mm in diameter was adopted for the strong polymers. Both indenters are much harder than the corresponding polymers, thus can be considered as rigid bodies for simplicity. The scratch length was set at 100 mm. A scratch velocity of 100 mm/s was employed for all rigid polymers. For the soft TPO, scratch tests were performed at scratch velocities of 1 and 100 mm/s, respectively. A normal load which is linearly increased with scratch distance was imposed on the scratch tip. The load range was from 1 N to 30 N and 1 N to 100 N for the weak and strong polymers, respectively; a lower load range of 0.5–7 N was employed for the soft TPO to prevent penetration of the scratch tip through the substrate.

2.3. Scratch damage analysis

For the purpose of promptly assessing the various surface scratch damage features, the images of scratched samples were acquired using the Epson 4870 Perfection Photo flatbed PC scanner at 3200 dpi resolution. Optical microscopy (OM, Olympus BX60) and scanning electron microscopy (SEM, JEOL JSM-6400) were then adopted to investigate the detailed scratch damage mechanisms.

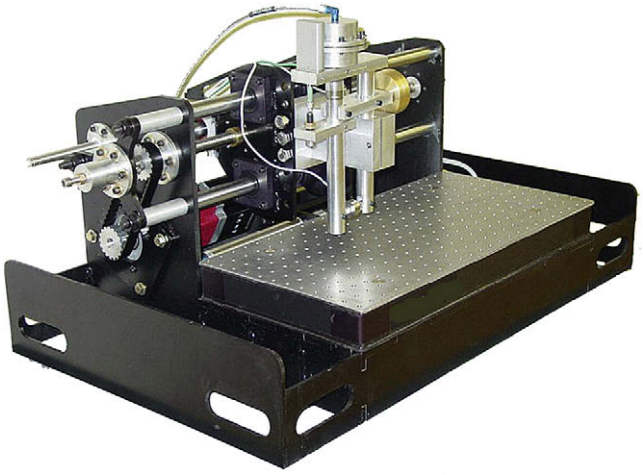

Fig. 2. A custom-built scratch machine to carry out the ASTM/ISO standard tests.

3. Finite element analysis

Due to the significant localized deformation during the scratch process, the stress and strain states experienced by the polymer substrate are extremely complex. To understand the mechanistic origins behind the observed scratch damage features, 3D FE analysis was performed to simulate the process of steel tip scratching on a ductile polymer using ABAQUS/Explicit® [34].

The dimensions of the FE model were 50 mm in length, 10 mm in width, and 3 mm in thickness. A scratch tip having a spherical diameter of 1 mm was modeled as an analytical rigid surface. To correlate with the details on the scratch-induced damage features, a fine FE mesh was adopted for the analysis with 512 elements over the scratch path as shown in Fig. 3 [28]. Eight-node tri-linear elements with three nodal displacement degrees of freedom and reduced integration were chosen as the substrate elements with a typical size of 0.05 mm by 0.05 mm by 0.05 mm. All the nodes on both ends were restrained from movement in all directions to simulate the clamping of the specimen during testing. All the nodes on the bottom surface were restrained vertically to model the stage support of the test specimen. A small normal load of 0.04 N was applied at the beginning to maintain substantial surface contact between the tip and substrate, followed by a linear increasing normal load up to 30 N at a scratch distance of 100 mm.

Since the current FEM simulation assumes that there is no crack formation, i.e., no nodes and elements separation, throughout the model, the simulation results are only valid up to the onset of cracking/crazing formation. Consequently, the qualitative trends for the evolutions of von Mises stress, maximum principal stress, dilatation, scratch depth, and scratch width as a function of the applied normal loads for the four different categories of polymer types would be similar. Therefore, there is only a need to perform FEM modeling work based on one polymer type. In this study, a typical ductile TPO was chosen for the simulation work.

For a ductile TPO material, similar to an earlier work [35], a piecewise linear stress–strain curve was constructed based on experimental data (Fig. 4). The stress softening and strain hardening characteristics are clearly illustrated. The coefficient of friction between the tip and TPO surface was taken to be 0.3 [19]. A 3D dynamic and plastic stress analysis mode was executed. To avoid excessive element distortion, adaptive remeshing was adopted to preserve the mesh quality. It should be noted that, elements separation or removal after damage was not considered in the current FEM modeling. Therefore, the modeling work can only simulate material deformation up to the onset cracking/crazing formation.

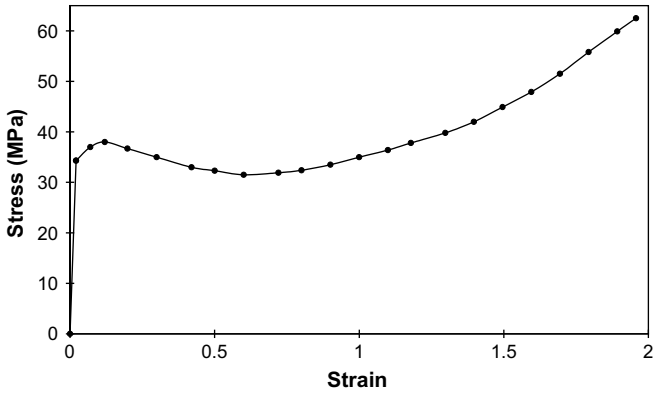

Fig. 4. Piecewise linear stress–strain curve for a model TPO.

4. Scratch damage modes and their evolution process

The polymer scratch damage mechanisms and their evolution process are quite different for the four polymer types at different load levels. To assist fundamental understanding of polymer scratch behavior, phenomenological categorization of the scratch damage modes is necessary. Furthermore, the understanding of the damage evolution process as a function of the increasing normal loads and the corresponding stresses is also critical for the correlation between scratch behavior and material parameters.

4.1. Categorization of scratch damage mode

4.1.1. Initial damage zone

For all materials tested, there is only a small amount of deformation observed under a low load and stress level. This includes fully recoverable elastic deformation, time-dependent viscoelastic deformation, and a small amount of non-recoverable plastic deformation resulting from compressive indentation, tentatively termed "mar". It is noticed that for polymers such as epoxy and PC, the initial damage induced by scratch is practically undetectable until a relatively high normal load is applied because of their high strength and elastic recovery against deformation. On the other

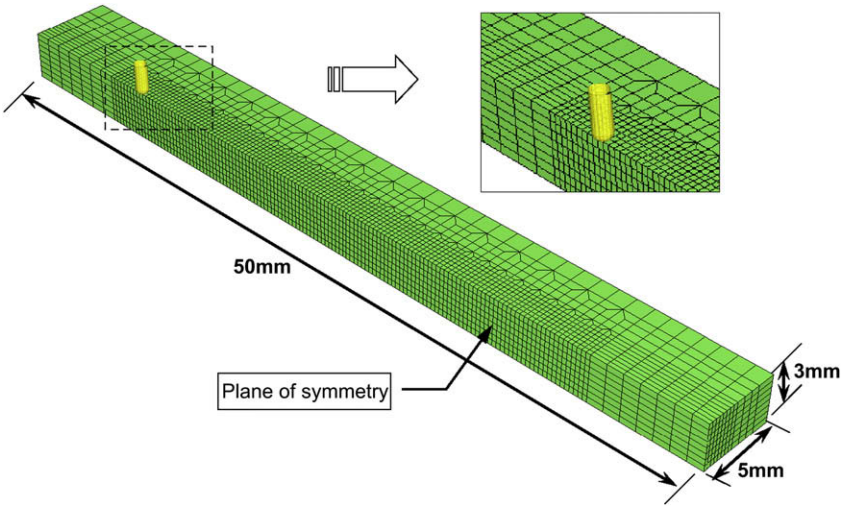

Fig. 3. FE model for polymer scratch simulation [28].

hand, polymers such as PS and TPO may exhibit various forms of scratch-induced localized small scale damage in this zone, including ironing and surface roughening, etc.

4.1.2. Fish-scale zone

With an increasing scratch normal load, the TPO substrate begins to undergo plastic deformation, forming a periodic concave damage feature pointing toward the scratch direction. Fig. 5(a) illustrates this scratch damage mechanism at the transition from the initial damage zone to the fish-scale damage of TPO. If the normal load is further increased, the fish-scale damage can become a well-developed, repeatable pattern as presented in Fig. 5(b). The fish-scale damage is dominated mostly by the plastic drawing of substrate material under the tip and is one of the most widely observed phenomena for polypropylene-based polymers [3–6].

For PS, a barely detectable pseudo fish-scale pattern is found to coexist with micro-scale cracks or voids. This damage feature is shown in Fig. 5(c).

4.1.3. Parabolic crack zone

For PC and Epoxy, except for the sporadic localized damage, which is formed due to presence of dust particles or local defects on the surface, there is no other observable scratch-induced damage until a high normal load of 70 and 75 N for PC and Epoxy, respectively. At this point, parabolic cracks begin to form and become the dominant damage mode. This kind of periodic convex damage feature pointing opposite the scratch direction can be identified as either a typical brittle damage feature or a tearing damage. Fig. 6(a) illustrates the transitions from mar deformation to the parabolic crack zone for Epoxy. Due to the brittle nature of the material, the cracks propagate promptly in a brittle fashion once they are formed. One can clearly find that this parabolic brittle damage feature becomes more regular and dense with an increasing scratch load. Similar parabolic cracks are also observed in ceramics, glass, and even metal materials [36–39].

For PC, the transition from mar damage to the parabolic crack zone is shown in Fig. 6(b). Here, the parabolic crack damage is slightly different from those formed in brittle matrices, such as epoxy. It appears that once the crack initiates, the crack opens up without significant extension. This is indicative of the ductile nature of PC.

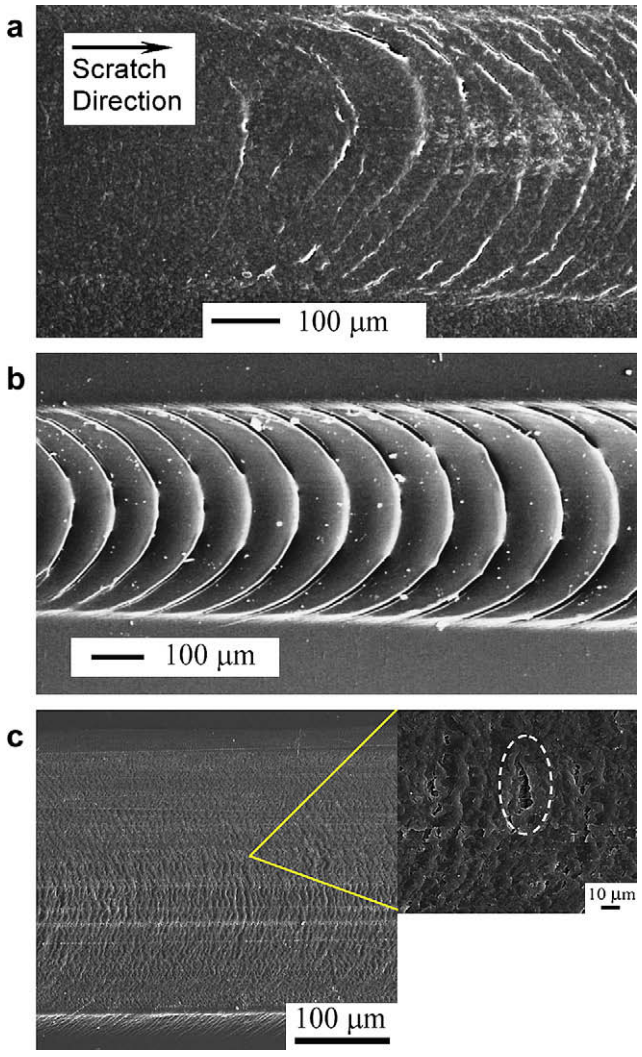

Fig. 5. SEM of fish-scale damage: (a) onset of fish-scale formation for TPO; (b) well-developed fish-scale for TPO; and (c) pseudo fish-scale pattern mixed with crazes/voids for PS.

4.1.4. Material removal zone

Ultimately, material removal will occur when the scratch load continues to increase. In the material removal zone, the tip penetrates through the top surface of the substrate and the significant material is removed from the surface. Fig. 7(a) shows the transition from the well-developed fish-scale zone to the rupture of this repeated fish-scale pattern, leading to material removal of TPO. Fig. 7(b) shows the transition from the pseudo fish-scale pattern mixed with crazes/voids to the material removal of PS. For PC, the transition from the parabolic crack zone to the material removal zone is shown in Fig. 7(c). Although this type of damage was not observed in epoxy in the current test condition, it is expected that material removal will occur if the applied load is high enough.

4.2. Evolution map of scratch damage modes

For the four categories of polymers, the evolution process of scratch damage with increasing normal load is quite different and is schematically illustrated in Fig. 8.

4.2.1. Ductile and strong material

For ductile and strong polymers, which exhibit high tensile strength and high ductility, only minor mar damage has a chance to occur under a low scratch load. Since the modulus and yield strength of this category of polymer are generally high, the scratch penetration depth is low. As a result, the resistance force against the tip movement from the material pile-up in front of tip remains low. The scratch coefficient of friction (μ_s), which can be divided into two parts: a traditional surface contact friction and an additional coefficient term resulting from the resistance of the material pile-up, stays low. Based on our previous studies [18–20,33], the smaller μ_s is, the better the scratch resistance is obtained. Not until an extremely high load is applied will the tip penetration become high enough to cause a dramatic increase in μ_s.

As observed, the occurrence of parabolic ductile tearing cracks is the most prevalent damage mode under a high normal load for PC. For other strong polymers that are more ductile and exhibit milder strain hardening characteristics (see also FEM modeling analysis below), it is anticipated that the ductile-type fish-scale damage will prevail.

4.2.2. Ductile and weak material

For ductile and weak polymers, which exhibit low tensile strength but high ductility, mar damage will occur first under a low scratch load. Then, the ductile fish-scale damage becomes the most favorable damage mode and will become well-developed with

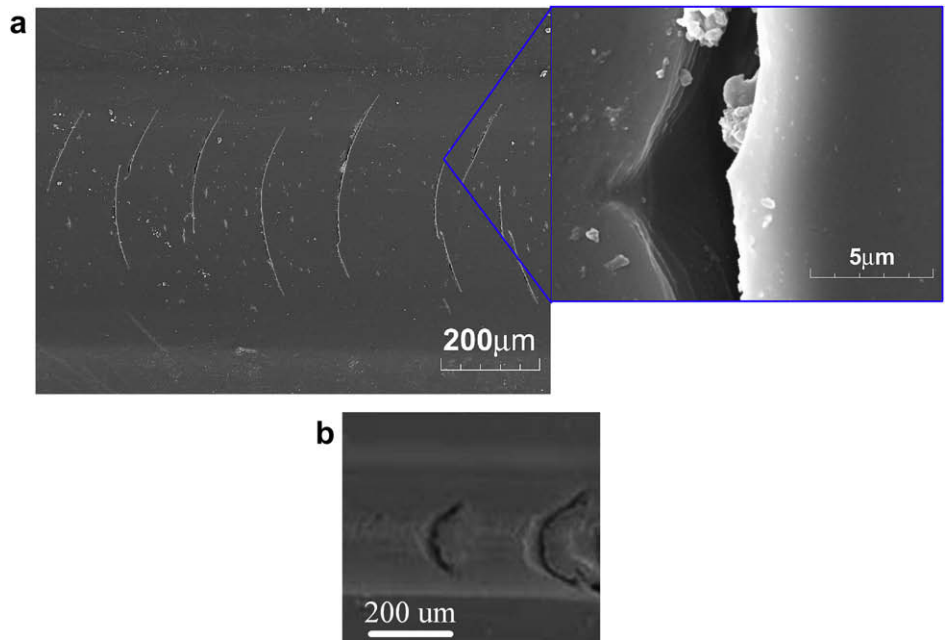

Fig. 6. SEM of parabolic crack pattern in: (a) Epoxy; and (b) PC.

increasing scratching load. With further increase in scratching load level, material removal takes over to rupture the well-developed fish-scale pattern. Finally, significant material removal takes place from its surface.

4.2.3. Brittle and weak material

For brittle and weak polymers, which exhibit low tensile strength and low ductility, small scale damage will occur even at low loads. As the scratching load level increases, scratch-induced damage will occur in the form of a mixture of pseudo fish-scale and microcracks, crazes or voids. At a high level of scratch load, material removal takes place in an irregular manner.

4.2.4. Brittle and strong material

Similarly, mar damage occurs at a low load for this type of material. In spite of its brittleness, a high scratching load level is required to develop any detectable damage. Parabolic cracks will eventually form after the scratching load reaches a certain magnitude. Epoxy which exhibits low tensile ductility but high compressive strength and ductility is a good example of this type of material. As expected, ceramics and glass fall into this category of material type and similar scratch behaviors have been observed [36–39].

4.3. Rate effect on polymer scratch damage

To study how the rate of testing influences the scratch-induced damage mechanisms, a TPO containing 70 wt% of EPR rubber and 30 wt% PP, also termed soft TPO, was chosen. Soft TPO has been shown to exhibit high rate-sensitivity [25]. Its apparent tensile strength increases from 0.75 MPa to 1.78 MPa and the elongation at break drops from 170% to 120% when the rate of tensile test increases from 0.083 mm/s to 8.3 mm/s [25]. The faster the rate of testing is, the more the scratch behavior will resemble a rigid brittle material.

The scratch-induced damage features of the soft TPO at different scratch rates are shown in Fig. 9. At 1 mm/s of scratch testing rate, the soft TPO is categorized as ductile and weak material and the fish-scale type of damage is clearly observed and is well-developed (Fig. 9(a)). At 100 mm/s of testing rate (Fig. 9(b)), it is categorized as

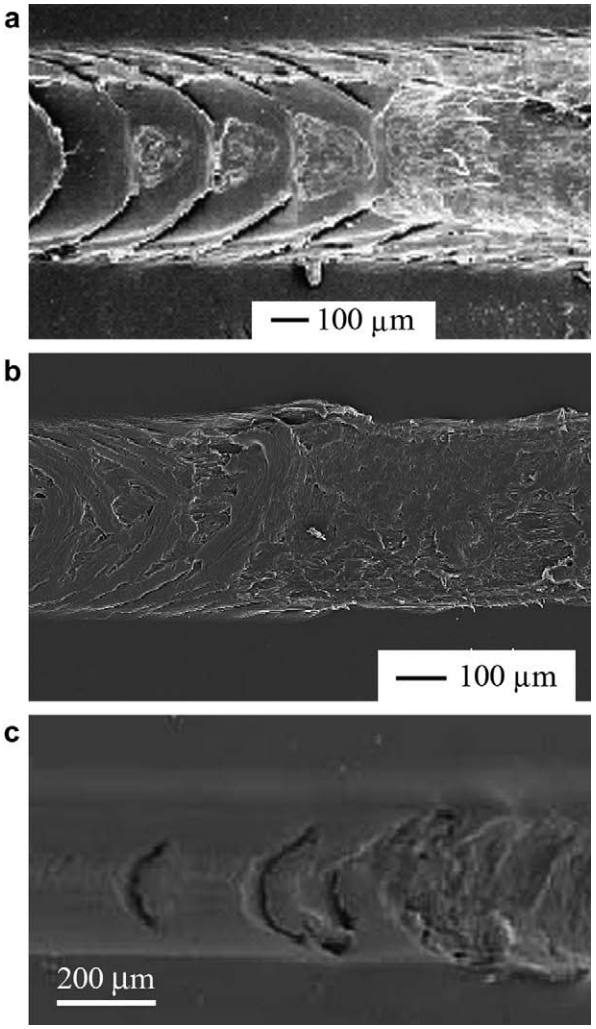

Fig. 7. SEM of the onset material removal region in (a) TPO; (b) PS; and (c) PC.

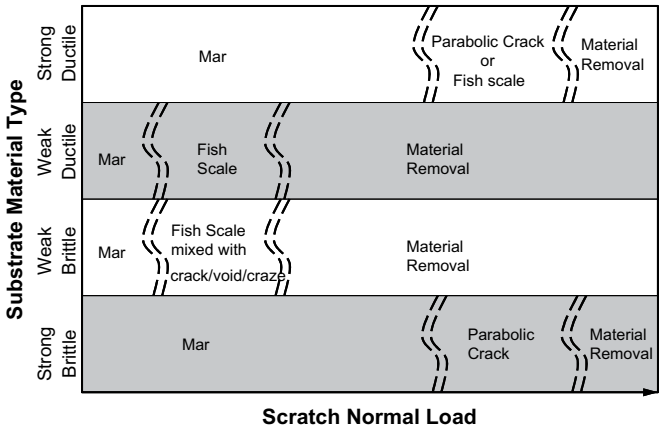

Fig. 8. Evolution map of polymer scratch damage.

brittle and weak at a high testing rate and only pseudo fish-scales mixed with proto-crazes or cracks are found, which is similar to what is observed in PS (Fig. 5(c)).

It is worth noting that both the testing rate and temperature can have significant influences on material mechanical responses, thus their scratch behaviors. When categorizing the polymer type, both testing rate and temperature should be considered; they may influence scratch damage modes even for the same material, as in the soft TPO case.

5. Evolution of scratch damage mechanisms

It is important to note that, during the ASTM/ISO based linearly increasing normal load scratch test, the stress and strain magnitudes exerted along the scratch path do not increase linearly, even for linear elastic materials [5]. For polymers with complex material constitutive behaviors, the development of stress and strain fields throughout the scratch test is inevitably much more complicated and can only be described numerically. To elucidate the evolution of the scratch damage formation, numerical analysis, such as FEM, is essential.

5.1. Stress analysis

The maximum principal stress contours and their orientations under low, moderate and high scratching normal loads are plotted in Fig. 10. Here, only the top layer of the material elements is plotted and the scratch tip is removed for better visualization. The location of the tip center is indicated by the bold arrow.

The material beneath the front portion of the scratch tip (region A) always experiences a compression. The compressive stress magnitudes are 23, 34 and 37 MPa for the applied normal loads of 8, 14 and 20 N, respectively. Meanwhile, a maximum principal stress of 17 MPa under the normal load of 8 N is developed behind the scratch tip (region B) and increases to 35 and 40 MPa as the normal load is further increased to 34 and 37 N, respectively. As has been shown in an actual scratch test and the numerical simulation here, the material is raised in front of the scratch tip during the scratch process (region C). As the applied normal load is further increased, another barely noticeable tensile region under small normal loads has now become significant here. It increases to 18 and 48 MPa at normal loads of 14 and 20 N, respectively, and develops as another possible region for the formation of brittle type of scratch damage.

Due to the scratch tip movement, the material in front of the tip quickly transits from a tensile condition (region C) to a compressive condition (region A), and then back to a tensile condition (region B). Inherent to the polymer scratch process, the scratch-induced damage mechanism(s) incurred will likely be influenced by the stress state, stress magnitude, and material characteristics the polymer experiences and possesses. These factors are discussed in detail below.

5.2. Ductile deformation vs. brittle damage

To study the different damage modes and their evolution processes with an increasing normal load, knowledge on the stress

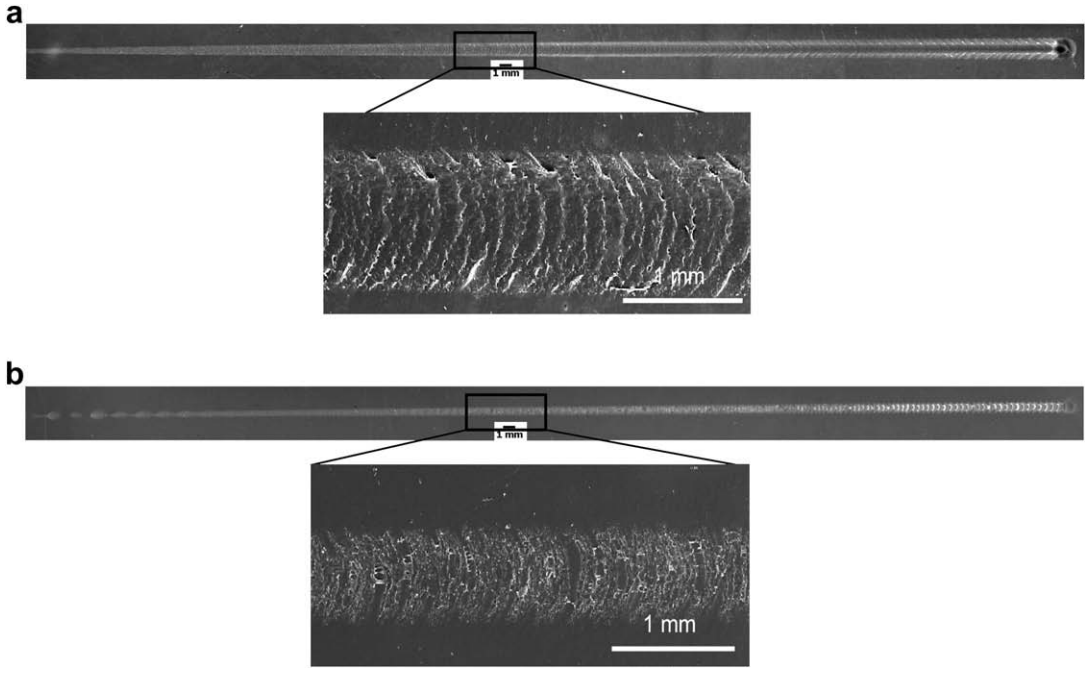

Fig. 9. Scratch damage of EPR-rich TPO at different testing rates of: (a) 1 mm/s; and (b) 100 mm/s.

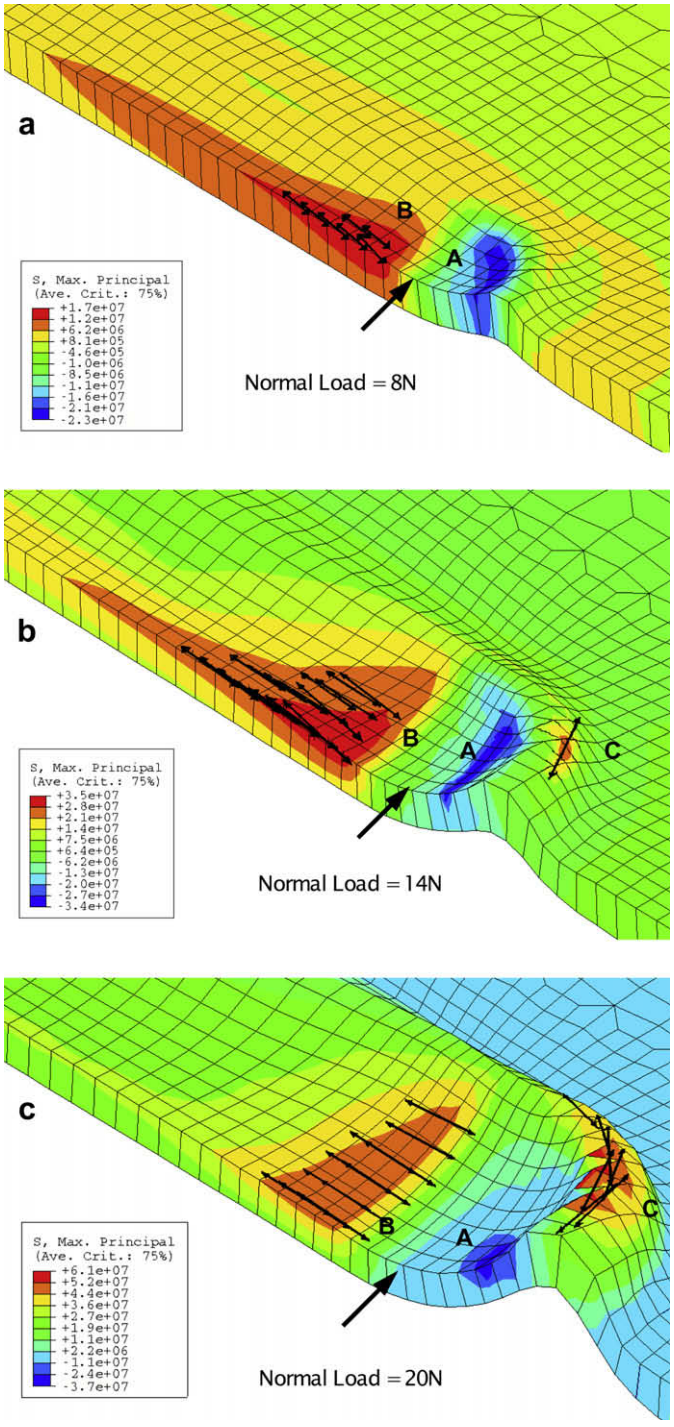

Fig. 10. Maximum principal stress contour plots at normal loads at: (a) 8 N, (b) 14 N, and (c) 20 N.

state and magnitude the material experiences near the scratch tip is necessary. The relationship between the scratch normal load and the von Mises stress at region A, which is closely related to the experimentally observed ductile deformation, is plotted in Fig. 11. To illustrate the size of the permanent deformation zone, the residual scratch depth and width are also presented in Fig. 11. It is noted that the FEM modeling here does not take into account of element separation or removal after damage. The scratch-induced deformation, which is reflected by the observed residual scratch depth and scratch width, will continue to evolve since the elements

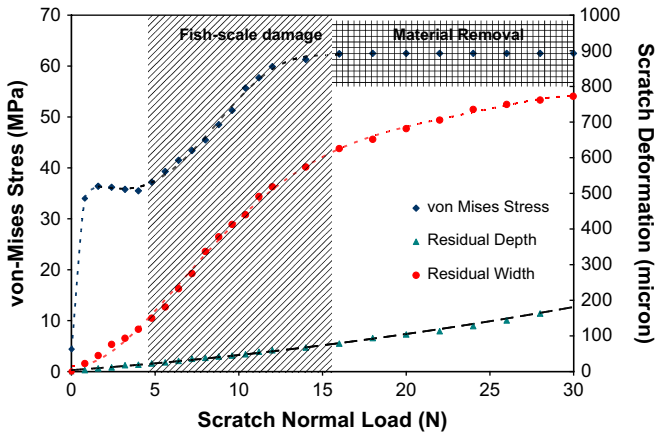

Fig. 11. von Mises stresses and residual scratch depths and widths as a function of applied normal load.

do not fail as the normal load is further increased. However, in reality, the material will fail and lead to material removal.

While the von Mises stress increases with the normal load from the very beginning and quickly reaches beyond the yield point under a relatively small normal load due to a small tip contact area, the scratch-induced plastic deformation is quite subtle at this stage, exhibiting only 20 μm of residual scratch depth and 120 μm of residual width at 5 N of normal load. This level of deformation is barely visible to the naked eyes. This is the reason why at most only mar damage can form at the beginning of the scratch process. When

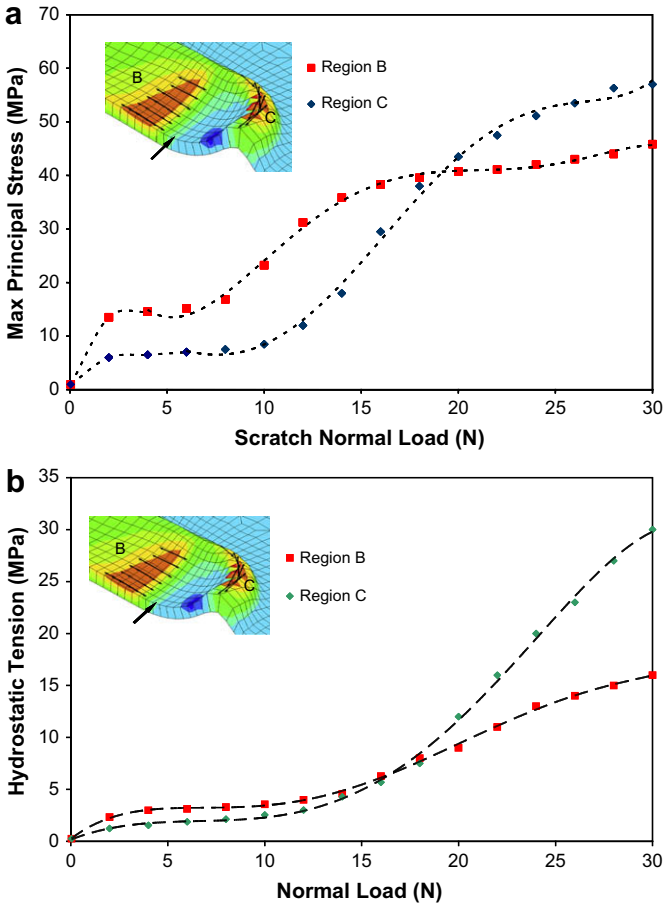

Fig. 12. Stress magnitude in regions B and C as a function of applied normal load: (a) maximum principal stresses and (b) hydrostatic tension.

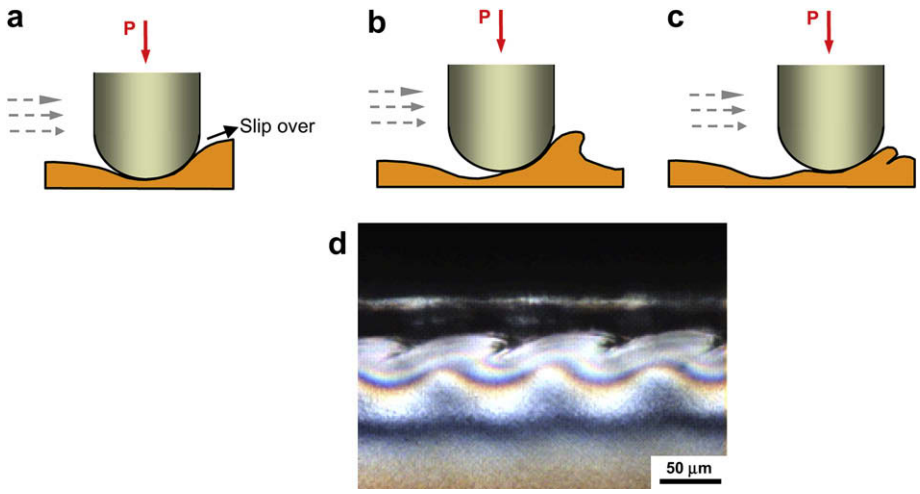

Fig. 13. Fish-scale formation mechanisms: (a) slipping, (b) drawing, (c) substrate compression, and (d) longitudinal section of OM of the fish-scale along the scratch path for TPO.

the applied normal load is increased, the von Mises stress magnitude will reach a maximum and drop slightly due to the strain softening nature of the polymer after yielding. Then, the stress magnitude increases again because of the strain hardening effect. The fish-scale damage tends to occur between the yielding and strain hardening region. Finally, the stress level reaches the ultimate strength of the material and the material removal process begins.

For the formation of brittle damage, the evolution of the maximum principal stress in regions B and C are plotted in Fig. 12(a). After an early increase of the maximum principal stress magnitude, it is found that the stress magnitude for both regions levels off to a low magnitude of 15 MPa and 6 MPa for regions B and C, respectively. The yielding related damage may dominate in this load range if the material is relatively ductile. The maximum principal stress magnitude then increase for both regions and the rate of increase slows down at a higher normal load range. When a moderate normal load is applied, the maximum principal stress magnitudes in regions B and C increase to such a magnitude that it can no longer be ignored. For brittle and weak polymers, cracking and voiding are favored now. Because of the higher maximum principal stress experienced in region B, the brittle types of damage mechanisms tend to occur there first, which leads to the formation of the parabolic crack zone observed in PC and Epoxy. Under a high level of normal load, the maximum principal stress in region C becomes larger than that in region B. Consequently, brittle damage will dominate in region C, which resembles a cutting process.

Hydrostatic tension is known to be responsible for the volume increase within a material, thus is strongly related to the brittle damage mechanisms, such as cracking, crazing, voiding, and interfacial debonding [10,11]. To assess the probability of the occurrence and location of brittle damage, the hydrostatic tension components in regions B and C were also plotted to address the possible brittle damage during scratch (Fig. 12(b)). Similar to the maximum principal stress trends, it is found that the hydrostatic tension levels off to about 3 MPa and 2 MPa in regions B and C, respectively, after an initial sharp increase. Given the high von Mises stress magnitude and the low hydrostatic tension level in the early stage of scratch, ductile yielding is likely to dominate. However, if the polymer is brittle and weak, cracking, crazing, and other types of brittle damage may still take place at low loads. When the applied normal load is further increased, the hydrostatic tension magnitude begins to increase significantly and help facilitate the formation of brittle damage. For the strong polymers, brittle types of damage become more dominant as the applied normal load is further increased. It is likely that the material removal will take place at this later stage, which has been experimentally observed (Fig. 6).

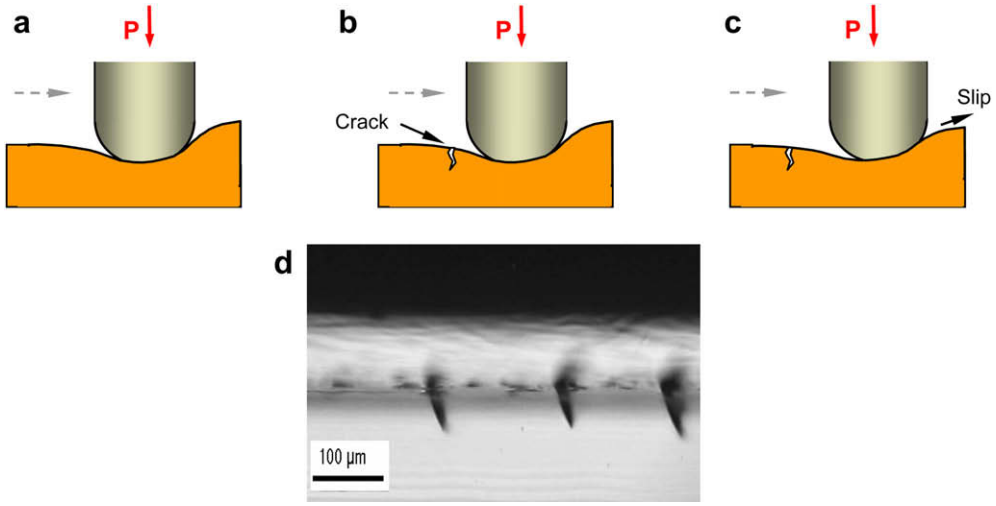

Fig. 14. Parabolic crack formation mechanisms: (a) stick, (b) crack formation, (c) slip, and (d) longitudinal-section OM of the parabolic crack along the scratch path for epoxy.

The competition between ductile deformation and brittle damage always exists throughout the entire scratch process. Depending on the material properties, i.e., ductile vs. brittle and strong vs. weak, and the corresponding stress state and magnitude under the prescribed loading conditions, either ductile deformation or brittle damage will become the dominant damage mechanism. The above factors are responsible for the various damage modes observed during polymer scratch. Extensive research efforts are still needed to understand the scratch behavior of polymers exhibiting different constitutive behaviors.

5.3. Scratch-induced periodic damage features

For all the scratch tests performed, regardless of the type of damage mode involved, the same damage feature will usually repeat itself until the normal load level is high enough to trigger the next damage mode. To explain this periodic occurrence of scratch damage, it is necessary to analyze the scratch process in a greater depth.

When the scratch tip ploughs through the material ahead of it, the material will be either pushed forward or piled up sideways [31]. This phenomenon is usually observed for relatively ductile polymers, where ironing and plastic deformation take place readily. In addition to the surface friction between the substrate and the scratch tip, the material accumulated ahead of the tip also introduces resistance against the tip movement [19]. An increased normal load causes deeper tip penetration into the substrate (Fig. 13(a)), which causes further increase of frictional force. In turn, the tip will drag the material along with it during scratch (region B in Fig. 10). When the induced stress magnitude becomes greater than the onset value for yielding, the fish-scale damage pattern will be formed through plastic drawing of the material (Fig. 13(b)). Eventually, the exerted tensile stress will become high enough to cause the next stage of scratch damage – material removal.

The "stick-slip" phenomenon [40,41] occurs when the indenter experiences periodic changes in resistance during the tip movement. The scratch tip is designed to move at a constant speed. However, the actual velocity of the tip movement relative to the material surface oscillates due to the physical nature of surface contact between a non-rigid tip and the substrate, where formation and breakage of a local scale adhesion between tip and material occur repeatedly. When the velocity of the tip relative to the material surface drops, the sticking phenomenon occurs. This phenomenon becomes more significant when the tip penetrates deep in the substrate, which introduces additional resistance force. The stored strain energy continues to build up due to the increasing applied normal load and the inertia exerted from the fixed testing rate (Fig. 13(a)). If the exerted stress on the material is lower than the ultimate strength of the material, the scratch tip will drag the material along (Fig. 13(b)) and slip over the ridge of the pile-up region (Fig. 13(c)). The tip may lose its full contact with the material surface during the slip process. Because of the decrease in resistance for the tip movement, the tip can push forward in full speed again. By the sheer action of the applied normal load, the scratch tip will soon reestablish its surface contact and begin to compress the material again. The stick stage occurs again until the next slipping action repeats itself.

Two possible mechanisms are involved in the stick-slip step. For ductile and weak polymers, the repeated surface contact and substrate compression by the scratch tip after each stick-slip step introduces the observed periodic damage feature. An OM image of a longitudinal section along the scratch path of TPO is shown in Fig. 13(d). The repeated fish-scale mechanism can be easily observed. Meanwhile, for brittle and strong polymers, a similar strain energy accumulation during the stick step occurs (Fig. 14(a)). Before the indenter loses its full contact with the substrate and slips over as described above, the tensile stress magnitude in the region behind the scratch tip may have already reached its ultimate strength. Thus, brittle fracture takes place to release the accumulated strain energy. Afterwards, the resistance decreases. Thus, the tip can slip over and move again (Fig. 14(b) and (c)). The repeated energy release process by the brittle damage behind the tip leads to the formation of the observed parabolic crack zone. The longitudinal section along the scratch path of the model epoxy clearly shows this type of damage caused by the scratch tip stick-slip phenomenon (Fig. 14(d)). It is noted that, due to the brittle nature of the material, the parabolic crack formation of brittle polymers rapidly propagates after it is initiated; the release of the strain energy accumulated from stick-slip process leads to a typical brittle feature. For those ductile and strong polymers, once the crack is initiated in a similar fashion, the subsequent process of strain energy release appears to be ductile tearing of the crack, which opens up the crack as observed in PC (Fig. 6(b)).

For the brittle and weak polymers, the fish-scale pattern cannot be well-developed because of the easy formation of brittle damage before the slip over. Instead, numerous microcracks, crazes, and/or voids are formed. The pseudo fish-scale contains a mixture of proto-cracks, crazes, or voids.

Under a high normal load level, large tensile stress magnitude will induce brittle damage as a dominant damage feature as discussed in the above section. The scratch tip can easily move forward directly through the pile-up, resembling a plowing process. Material removal due to the brittle damage is observed.

It is shown herein that the periodic scratch damage phenomena induced by the stick-slip process is not only related to the adhesive forces between the indenter and the substrate but also to the material type, indenter shape, scratch speed, and applied normal load. At low normal loads, where there is little material accumulation, the stick-slip steps are easily overcome by the inertia of the tip movement and by the low kinetic frictional resistance of the surface. With a larger normal load imposed onto the material, the scratch depth increases and more material builds up around the indenter. Hence, the stick-slip process becomes more dominant and must be accounted for. Research effort on the mechanics responsible for the observed stick-slip during scratch is now underway and will be reported in the near future.

Based on the knowledge gained above, it becomes clear how the material properties, the stress state, and its magnitude are profoundly important to affect the scratch-induced damage mechanisms. It is possible to promote or suppress certain damage mechanisms exerted by scratch. Depending on the scratching load expected and the type of material utilized, one can begin to predict the material properties needed to prevent the formation of undesirable scratch damage mechanisms. Quantitative assessment of the above idea is now underway and will be reported shortly.

6. Conclusions

The linearly increasing normal load scratch test, based on ASTM and ISO standards, has been performed on four categories of polymers: (I) ductile and strong, (II) ductile and weak, (III) brittle and weak, and (IV) brittle and strong. Various scratch damage modes have been identified for different polymer types. The scratch damage modes and evolution process with respect to the normal load level are described and discussed for each material category. A scratch damage evolution map has been constructed based on the above findings. The rate effect on polymer scratch has also been studied. With an aid of FEM modeling, the relationships among the scratch damage modes and their evolution, material type, testing rate, and applied scratch load have been discussed. The stick-slip process during polymer scratch is found to be responsible for the

observed periodic fish-scale pattern and parabolic crack formations. A better understanding of polymer scratch phenomena is gained, which, in turn, can be utilized to identify the material properties needed to prevent undesirable scratch damage mechanisms.

Acknowledgments

The authors would like to thank the financial support provided by the Texas A&M Scratch Behavior Consortium (Advanced Composites, Atlas-MTS, Braskem, Cabot, Ciba Specialty Chemical, Clorox, Dow Chemical, Japan Polypropylene, Kaneka, Rio Tinto, Phillips-Sumika, Solvay Engineered Polymers, Sumitomo Chemical, Surface Machine Systems, and Visteon) in this research endeavor. The authors would also like to acknowledge partial financial supports of the Department of Transportation (DTPH56-06-T-000022) and Defense Logistic Agency (SP0103-02-D-0003). Special thanks are also given to Ehsan Moghbelli and Goyteck Lim for their valuable discussion and generation of some figures.

References

[1] ASTM International, ASTM D7027–05; 2005.
[2] International Organization for Standardization, ISO 19252:2008; 2008.
[3] Wong M, Lim GT, Moyse A, Reddy JN, Sue H-J. Wear 2004;256(11–12):1214–27.
[4] Wong M, Moyse A, Lee F, Sue H-J. Journal of Materials Science 2004; 39(10):3293–308.
[5] Xiang C, Sue H-J, Chu J, Coleman B. Journal of Polymer Science, Part B: Polymer Physics 2001;39:47–59.
[6] Chu J, Xiang C, Sue H-J, Damon HR. Polymer Engineering and Science 2000;40(4):944–55.
[7] Xiang C, Sue H-J, Chu J, Masuda K. Polymer Engineering and Science 2001; 41(1):23–31.
[8] Vingsbo O, Hogmark S. Wear 1984;100:489–502.
[9] Liang YN, Li SZ, Li DF, Li S. Wear 1996;199:66–73.
[10] Atkins AG, Mai Y-W. Elastic and plastic fracture – metals, polymers, ceramics, composites, biological materials. Chichester: Ellis Horwood Ltd.; 1985.
[11] Kinloch AJ, Young RJ. Fracture behavior of polymers. New York: Elsevier Science Pub. Co.; 1983.
[12] Grasmeder JR. Polypropylene. Institute of Polymer, The International Conference; 1994. p. 98–108.
[13] Briscoe BJ, Pelillo E, Ragazzi F, Sinha SK. Polymer 1998;39(11):2161–8.
[14] Briscoe BJ, Delfino A, Pelillo E. Wear 1999;225:319–28.
[15] Tang H-X, Martin DC. Journal of Material Science 2003;38(4):803–15.
[16] Hiromi K, Maki M, Tsunetoshi K, Takashi K. ANTEC Annual Technical Conference Proceedings 2004;2:1938–42.
[17] Hadal RS, Misra RDK. Materials Science and Engineering: A 2005;398(1–2): 252–61.
[18] Ducret S, Pailler-Mattéi C, Jardret V, Vargiolu R, Zahouani H. Wear 2003; 255(7–12):1093–100.
[19] Jiang H, Browning R, Moyse A, Sue H-J. Applied Surface Science 2008;254: 4494–9.
[20] Browning R, Lim G, Moyse A, Sun L, Sue H-J. Polymer Engineering and Science 2006;46(5):601–8.
[21] Moghbellia E, Browning RL, Boo W-J, Hahn SF, Feick LJE, Sue H-J. Tribology International 2008;41:425–33.
[22] Moghbelli E, Sun L, Jiang H, Boo WJ, Sue H-J. Polymer Engineering and Science 2009;49:483–90.
[23] Briscoe BJ, Evans PD, Pelillo E, Sinha SK. Wear 1996;200:137–47.
[24] Briscoe BJ, Evans PD, Biswas SK, Sinha SK. Polymer Engineering and Science 1996;36(24):2996–3005.
[25] Bull SJ. Tribology International 1997;30(7):491–8.
[26] Jardret V, Morel P. Progress in Organic Coatings 2003;48:322–31.
[27] Browning RL, Jiang H, Moyse A, Sue H-J, Iseki Y, Ohtani K, et al. Journal of Materials Science 2008;43(4):1357–65.
[28] Brostow W, Hinze JA, Simoes R. Journal of Materials Research 2004;19(3):851–6.
[29] Zhang J, Sun T, Yan Y, Liang Y. Materials Science and Engineering A 2009; 505(1–2):65–9.
[30] Bucaille JL, Felder E. Philosophical Magazine A: Physics of Condensed Matter, Structure, Defects and Mechanical Properties 2002;82:2003–12.
[31] Lim GT, Reddy JN, Sue H-J. In: Urban M, editor. Stimuli-responsive polymeric films and coatings. ACS Symposium Series, 912; 2005. p. 166–80 [chapter 10].
[32] Pelletier H, Gauthier C, Schirrer R. Proceedings of the Institution of Mechanical Engineers, Part J: Journal of Engineering Tribology 2008;222:221–30.
[33] Jiang H, Lim GT, Whitcomb JD, Sue H-J. Journal of Polymer Science, Part B: 2007;45:1435–47.
[34] ABAQUS® analysis user's manual ver. 6.4. Pawtucket, Rhode Island: ABAQUS®, Inc; 2003.
[35] Sue H-J, Yee AF. Polymer 1988;29(9):1619–24.
[36] Li K, Shapiro Y, Li JCM. Acta Materialia 1998;46(15):5569–78.
[37] Lawn BR, Wiederhorn SM, Roberts DE. Journal of Material Science 1984; 19(8):2561–9.
[38] Ramasamy S, Mark J, Kiyoshi H, Kanemastsu W. Journal of European Ceramic Society 2006;26(3):351–9.
[39] Hodge AM, Nieh TG. Intermetallics 2004;12(7–9):741–8.
[40] Li K, Ni BY, Li JCM. Journal of Material Research 1996;11(6):1574–80.
[41] Zhang SL, Li JCM. Materials Science and Engineering: A 2003;344(1–2):182–9.